

LEWIS  
NOSC

NOSC TR 496

DTIC  
ELECTED  
S JUN 27 1980  
C D

Technical Report 496

NOSC TR 496

**TORPEDO HYDRODYNAMIC PARAMETER  
ESTIMATION: APPLICATION TO SHALLOW  
WATER MOBILE PLATFORM (SWAMP)  
SEA RUN DATA**

FILE COPY ADA086028

L. A. Lopes

1 February 1980

Approved for public release; distribution unlimited

NAVAL OCEAN SYSTEMS CENTER  
SAN DIEGO, CALIFORNIA 92152

80 6 27 012



NAVAL OCEAN SYSTEMS CENTER, SAN DIEGO, CA 92152

---

AN ACTIVITY OF THE NAVAL MATERIAL COMMAND

SL GUILLE, CAPT, USN

Commander

HL BLOOD

Technical Director

ADMINISTRATIVE INFORMATION

The work described in this report was performed under the NOSC IR/IED program, work unit ZR97, during FY 79. The SWAMP program, which collected the data used in this work between March 1977 and July 1978, was supported by the Shallow Water G&C Block and the Weapons Environment Support Program with funds administered by the Naval Sea Systems Command.

Released by  
Dr. J. C. Reeves, Head  
Weapons Technology Division

Under authority of  
R. H. Hearn, Head  
Fleet Engineering Department

REPORT DOCUMENTATION PAGE		READ INSTRUCTIONS BEFORE COMPLETING FORM
1. REPORT NUMBER NOSC Technical Report 496 (TR 496)	2. GOVT ACCESSION NO. AID-AC86028	3. RECIPIENT'S CATALOG NUMBER
4. TITLE (and Subtitle) TORPEDO HYDRODYNAMIC PARAMETER ESTIMATION: APPLICATION TO SHALLOW WATER MOBILE PLATFORM (SWAMP) SEA RUN DATA.	5. TYPE OF REPORT & PERIOD COVERED Research report, March 1977 - September 1979	
6. AUTHOR(s) L. A. Lopes	7. CONTRACT OR GRANT NUMBER(s)	
8. PERFORMING ORGANIZATION NAME AND ADDRESS Naval Ocean Systems Center San Diego, CA 92152	10. PROGRAM ELEMENT, PROJECT, TASK AREA & WORK UNIT NUMBERS NOSC IR/IED Program, work unit ZR97	
11. CONTROLLING OFFICE NAME AND ADDRESS 1234	11. REPORT DATE 1 Feb 1980	
14. MONITORING AGENCY NAME & ADDRESS (if different from Controlling Office)	12. NUMBER OF PAGES 30	
16. DISTRIBUTION STATEMENT (of this Report)	15. SECURITY CLASS. (of this report) Unclassified	
17. DISTRIBUTION STATEMENT (of the abstract entered in Block 20, if different from Report)	18a. DECLASSIFICATION/DOWNGRADING SCHEDULE	
18. SUPPLEMENTARY NOTES 14) NOSC/TR-496		
19. KEY WORDS (Continue on reverse side if necessary and identify by block number) Torpedoes Hydrodynamics Shallow Water Mobile Platform (SWAMP)	Computer modeling Parameter estimation	
20. ABSTRACT (Continue on reverse side if necessary and identify by block number) The Shallow Water Mobile Platform (SWAMP) is a specially instrumented torpedolike vehicle whose purpose is to gather acoustic research data. A model of SWAMP, based on torpedo motion equations with six degrees of freedom, is presented here. Multiplexed dynamic data employed include clock time, body angular rate components, control surface deflections, propeller rotation speed, vehicle course, and depth. First-order maximum likelihood identification algorithms are used as a guide in parameter estimation. These algorithms yield an estimation of the state of the system by means of an extended "Kalman"-type filter, as well as a weighted quadratic function of the residues (ie, differences between measurements and their computed values) as the maximum likelihood cost		

393159

Lia

UNCLASSIFIED

SECURITY CLASSIFICATION OF THIS PAGE (When Data Entered)

20. Continued.

function. The filter computes an estimate of the full SWAMP trajectory. A cost function is provided in the form of a weighted sum of squares of the residues of the rate gyros and accumulators. Of gradient techniques investigated for the minimization of the cost function, the Fletcher-Powell technique was found to be superior (as modified because of the extreme sensitivity of the roll-damping coefficient), and only results for this technique are presented.

UNCLASSIFIED

SECURITY CLASSIFICATION OF THIS PAGE (When Data Entered)

## PROBLEM

Model a specially instrumented, torpedolike Shallow Water Mobile Platform (SWAMP) vehicle for gathering acoustic research data.

## RESULTS

The SWAMP model was based on torpedo motion equations with six degrees of freedom. Multiplexed dynamic data employed included clock time, body angular rate components, control surface deflections, propeller rotation speed, vehicle course, and depth. First-order likelihood identification algorithms were used as a guide in parameter estimation. The algorithms yielded an estimation of the state of the system by means of an extended "Kalman"-type filter as well as a weighted quadratic function of the residues (ie, differences between measurements and their computed values) as the maximum likelihood cost function. Of gradient techniques investigated for the minimization of the cost function, a modified Fletcher-Powell technique was found to be superior.

## RECOMMENDATIONS

Further work on post-run analysis should include analysis of the data to estimate correlation matrices; improvement of the system model by identification of nonlinear effects in yaw, pitch, and roll coupling; and further development of digital recording and playback equipment for use in torpedo guidance and control development, test, and evaluation.

Accession For	
NTIS GEN&I	
DOC TAB	
Unannounced	
Justification	
By	
Distribution/	
Availability Codes	
Dist	Avail and/or
	special

## CONTENTS

1. INTRODUCTION ... page 3
2. THE RECURSIVE FILTER ... 4
3. APPLICATION TO SWAMP ... 5
4. SWAMP SEA RUN RESULTS ... 8
5. COST FUNCTION AND ITS MINIMIZATION ... 11
6. RESULTS ... 14
7. CONCLUSIONS AND RECOMMENDATIONS ... 26

REFERENCES ... 26

APPENDIX: FILTER EQUATIONS ... 27

## 1. INTRODUCTION

System identification, or modeling, is one of the problems considered by modern systems theory. It consists in determining a difference or differential equation, or the coefficient parameters of such an equation, so that it describes the evolution of a physical process in conformance with a specified criterion. The system that is considered in this report is the Shallow Water Mobile Platform (SWAMP); its model is the torpedo motion equations with six degrees of freedom, in finite difference form, in which the hydrodynamic coefficients (force and moment derivatives) are to be determined. Interest in the modeling of torpedoes had its origin during World War II. The problems that the Navy encountered with many submarine- and aircraft-launched weapons inspired research into torpedo dynamics and the establishment of hydrodynamic facilities for the testing of small-scale torpedo models and the measurement of hydrodynamic coefficients. Analytical methods based on these experimental data were also developed for estimating hydrodynamic coefficients of new torpedo configurations. The mathematical models that were formulated have been employed since then in the design of new torpedoes and in the prediction of their performance. Verification of simulation models has always been rather problematical. Sea run data have been recorded by oscillograph tracing on photographic film. Matching these records against a computer model has been accomplished by tweaking favorite parameters in the model until the response produced appeared visually to approximate the photographic record.

There was an analogous development in aircraft technology. However, new parameter estimation techniques began to be introduced in the mid 1960s. These techniques, which revolutionized estimation of aircraft flight parameters, were made possible by two factors: (1) highly automated data acquisition systems were becoming standard in flight testing; and (2) large high-speed digital computers were able to solve complicated algorithms efficiently. By 1973, this technology was widespread through the research field, so that a symposium on parameter estimation techniques and their application to aircraft flight testing could be held (reference 1).

The SWAMP is a specially instrumented torpedolike vehicle whose purpose is to gather acoustic research data. The dynamics data of the vehicle are recorded on a single channel of the same magnetic tape on which the acoustic data are recorded. These multiplexed data include a clock time, body angular rate components, body acceleration components, control surface deflections, propeller rotation speed, vehicle course, and depth. The rate gyros and accelerometers are in a Mk 46 control unit, and they are used for vehicle control. The data were sampled, digitized, and recorded at intervals of 23.04 milliseconds. The first-order maximum likelihood identification algorithms of reference 2 (see table 3.4-1 below) were used as a guide in the parameter estimation of this report. These algorithms yield an estimation of the state of the system by means of an extended "Kalman filter," as well as a weighted quadratic function of the residues (ie, differences between measurements and their computed values) as the maximum likelihood cost function. The weighting matrix of the cost is the inverse of the covariance matrix of the measurements. The filter used here

---

1. National Aeronautics and Space Administration TN D-7647, Parameter Estimation Techniques and Applications in Aircraft Flight Testing, April 1974.
2. Sage, A. P., and J. C. Melsa, System Identification, Academic Press, 1971.

is not a *true* Kalman filter. The state vector was partitioned, with part of the system being filtered by means of a constant-gain matrix. The gain matrix was obtained with some assumptions about the noise statistics and some experimentation with the filter. The remainder of the system was filtered in an *ad hoc* fashion. The filter computes an estimate of the full SWAMP trajectory. The cost function is a weighted sum of squares of the residues of the rate gyros and accelerometers. The weights were chosen according to a relative order-of-magnitude estimate of their variances. Various gradient techniques were investigated for the minimization of the cost function. The Fletcher-Powell technique (reference 2, chapter 4) was found to be superior to others that were tried, and only the results for this technique are presented. It was found necessary to introduce a modification of this method because of the extreme sensitivity of the roll-damping coefficient. The minimizing process had to restrict the range of this parameter to prevent instability.

## 2. THE RECURSIVE FILTER

As a model for the trajectory filter development, we follow the treatment by M. Aoki in reference 3. Suppose the system to be estimated has the evolution equation

$$\underline{x}_{i+1} = A_i \underline{x}_i + B_i \underline{U}_i + C_i \xi_i \quad (2.1)$$

where  $\underline{x}_i$  is the state vector at the  $i^{\text{th}}$  step,  $\underline{U}_i$  is the control vector at the  $i^{\text{th}}$  step, and  $\xi_i$  is a stochastic vector assumed to be a zero-mean, Gaussian random variable.  $A_i$ ,  $B_i$ , and  $C_i$  are matrices of appropriate dimensions. The measurement vector  $\underline{y}_i$  is given by

$$\underline{y}_i = H_i \underline{x}_i + \eta_i \quad (2.2)$$

where  $\eta_i$  is the measurement noise vector assumed to be also zero-mean Gaussian. It is assumed that  $\xi_i$  and  $\eta_i$  are independent and that covariance matrices are of the form

$$\text{cov}(\xi_i, \xi_j) = Q_i \delta_{ij} \quad (2.3)$$

$$\text{cov}(\eta_i, \eta_j) = R_i \delta_{ij} \quad (2.4)$$

$$\text{cov}(\xi_i, \eta_j) = 0 \text{ all } i, j \quad (2.5)$$

where  $\delta_{ij}$  is the Kronecker delta. The optimal estimate  $\underline{x}_i^*$  is given by

$$\underline{x}_{k+1}^* = \tilde{\underline{x}}_{k+1} + K_{k+1} (\underline{y}_{k+1} - H_{k+1} \tilde{\underline{x}}_{k+1}) \quad (2.6)$$

$$\tilde{\underline{x}}_{k+1} = A_k \underline{x}_k^* + B_k \underline{U}_k. \quad (2.7)$$

The filter gain  $K_{k+1}$  is defined by

$$K_{k+1} = P_{k+1} H'_{k+1} (H_{k+1} P_{k+1} H'_{k+1} + R_{k+1})^{-1} \quad (2.8)$$

where  $P_{k+1}$  is the *a priori* variance given by the evolution equation

$$P_{k+1} = A_k \Gamma_k A'_k + C_k Q_k C'_k \quad (2.9)$$

---

3. Aoki, M., Optimization of Stochastic Systems, Academic Press, 1967.

and

$\Gamma_k$  is the *a posteriori* variance recursively defined by

$$\Gamma_{k+1} = P_{k+1} - K_{k+1} H_{k+1} P_{k+1} \quad (2.10)$$

If  $Q_i$  and  $R_i$  are constant matrices independent of  $i$ , and  $A_i, H_i$ , and  $C_i$  are also independent of  $i$ , the filter gain reaches a steady-state value  $K$ . Moreover, if  $Q_i = \sigma^2 \tilde{Q}_i$  and  $R_i = \rho^2 \tilde{R}_i$ , then the steady-state value of  $P_i$  is proportional to  $\sigma^2$ , say  $P_i = \sigma^2 \tilde{P}_i$ . We then have the filter gain given by

$$K_i = \tilde{P}_i H_i' [H_i \tilde{P}_i H_i' + (\rho^2/\sigma^2) \tilde{R}_i]^{-1} \quad (2.11)$$

so that the steady-state gain depends only on the ratio of  $\rho^2$  and  $\sigma^2$ . If this ratio is chosen too large, the filter becomes unstable in correcting initial errors. A value was empirically determined that resulted in a stable filter and a smooth trajectory.

### 3. APPLICATION TO SWAMP

The equations of motion for the SWAMP vehicle are standard torpedo motion equations (reference 4). They govern the evolution of the components on the body-fixed axes of the linear velocity  $\underline{V}$  and the angular velocity  $\underline{\omega}$

$$\underline{V} = u \underline{i} + v \underline{j} + w \underline{k} \quad (3.1)$$

$$\underline{\omega} = p \underline{i} + q \underline{j} + r \underline{k} \quad (3.2)$$

where  $\underline{i}, \underline{j}, \underline{k}$  are unit vectors in the direction of the positive body  $x, y, z$  axes. The evolution of the other state variables, geographical coordinates of the vehicle CB, and vehicle orientation (Euler angles or direction cosines) is obtained by integration of the appropriate velocity components.

For the purpose of constructing a manageable filter, we have partitioned the state variables. Let the vector  $\underline{x}$  be defined as

$$\underline{x} = \begin{bmatrix} q \\ w \\ r \\ v \\ p \end{bmatrix} \quad (3.3)$$

Then the equations of motion give

$$\dot{\underline{x}} = \Phi(\underline{x}, \underline{U}) \quad (3.4)$$

where  $\underline{U}$  is a "control" vector containing the longitudinal speed component  $u$ , unbalanced roll torque  $K_o$ , control surface deflections  $\delta_e, \delta_U, \delta_L$ , and direction cosines of the gravitational vector  $G_1, G_2, G_3$ . We employ a fixed time step  $\Delta t$  and define

---

4. Naval Ordnance Test Station (Pasadena) NAVORD report 2090, Motion Equations for Torpedoes, by L. Lopes, 12 February 1954.

$$\begin{aligned}\underline{x}_k &= \underline{x} (k\Delta t) \\ \underline{U}_k &= \underline{U} (k\Delta t).\end{aligned}\quad (3.5)$$

Then, approximately,

$$\underline{x}_{k+1} = \underline{x}_k + \Phi(\underline{x}_k, \underline{U}_k) \Delta t. \quad (3.6)$$

Filter gain will be determined from the linearized equation, linearized about  $\underline{x} = \underline{0}$ ,  $\underline{U} = \underline{U}_0$ , corresponding to straight, level flight at constant speed.

$$\underline{x}_{k+1} = A\underline{x}_k + B\underline{U}_k \quad (3.7)$$

where

$$A = I + \Phi_{\underline{x}}(\underline{0}, \underline{U}_0) \Delta t \quad (3.8)$$

$$B = \Phi_{\underline{U}}(\underline{0}, \underline{U}_0) \Delta t. \quad (3.9)$$

The measurement vector is taken to be body rates as measured by rate gyros, so that

$$\underline{y}_k = \begin{bmatrix} q \\ r \\ p \end{bmatrix} = H\underline{x}_k \quad (3.10)$$

where

$$H = \begin{bmatrix} 1 & 0 & 0 & 0 & 0 \\ 0 & 0 & 1 & 0 & 0 \\ 0 & 0 & 0 & 0 & 1 \end{bmatrix}. \quad (3.11)$$

Comparing (3.7) with (2.1), we introduce the noise vector with the assumption that  $C_i$  is a constant diagonal matrix and  $Q_i = \sigma^2 I$ . Introducing measurement noise in (3.10), we assume  $R_i$  to be a constant-diagonal matrix. Equations (2.9) and (2.10) are then iterated to obtain a steady-state constant filter gain  $K$ . The filter is then given the form of the extended Kalman filter for nonlinear systems

$$\widetilde{\underline{x}}_{k+1} = \underline{x}_k^* + \Phi(\underline{x}_k^*, \underline{U}_k) \Delta t \quad (3.12)$$

$$\underline{x}_{k+1}^* = \widetilde{\underline{x}}_{k+1} + K(\underline{y}_k - H\widetilde{\underline{x}}_{k+1}). \quad (3.13)$$

The operator  $H$  will in fact be a matrix with differential operator elements accounting for the second-order rate gyro response and the limited output of the gyros.

Let us consider the "control" vector  $\underline{U}_k$  in more detail. The axial speed component  $u$  is governed by the longitudinal force equation which includes propeller thrust, vehicle drag, the axial component of the net buoyancy force, and centrifugal force terms. The propeller thrust is obtained from the empirically determined characteristics of the RETORC 1 propellers, and is a function of  $u$  and the propeller rotation speed. The vehicle axial drag is a function of  $u$ . The drag coefficient of the RETORC was modified to give the correct dive rate to the SWAMP vehicle. The measured control-surface deflections were fed directly into the motion equations. Random noise in these measurements will be filtered by the motion

equations. Vehicle orientation may be specified as in reference 4 by the Euler angles  $\psi, \theta, \varphi$  (course, pitch, and roll), or by the direction cosines of the vectors  $\underline{i}_0$  and  $\underline{k}_0$ , where  $\underline{i}_0$  is the horizontal vector in the direction of the gravitational force. From appendix E of reference 2, we have

$$\begin{aligned}\underline{i}_0 &= H_1 \underline{i} + H_2 \underline{j} + H_3 \underline{k} \\ \underline{k}_0 &= G_1 \underline{i} + G_2 \underline{j} + G_3 \underline{k}\end{aligned}$$

where

$$\begin{aligned}H_1 &= \cos \psi \cos \theta \\ H_2 &= \cos \psi \sin \theta \sin \varphi - \sin \psi \cos \varphi \\ H_3 &= \sin \psi \sin \varphi + \cos \psi \sin \theta \cos \varphi \\ G_1 &= -\sin \theta \\ G_2 &= \cos \theta \sin \varphi \\ G_3 &= \cos \theta \cos \varphi.\end{aligned}\tag{3.14}$$

The Euler angles may be recovered from these direction cosines as follows:

$$\begin{aligned}\varphi &= \tan^{-1} (G_2/G_3) \\ \theta &= \tan^{-1} \left( -G_1 / \sqrt{G_2^2 + G_3^2} \right) \\ \psi &= \tan^{-1} [\cos \theta (-H_2 \cos \varphi + H_3 \sin \varphi) / H_1].\end{aligned}\tag{3.15}$$

To emphasize the direction cosine formulation, we write  $\underline{i}_0 = \underline{H}$ ,  $\underline{k}_0 = \underline{G}$ . The evolution equations for  $\underline{H}$  and  $\underline{G}$  are

$$\begin{aligned}\dot{\underline{H}} &= \underline{H} \times \underline{\omega} \\ \dot{\underline{G}} &= \underline{G} \times \underline{\omega}\end{aligned}\tag{3.16}$$

which express the fact that they are fixed vectors relative to geographical coordinates. A predictor-corrector approach is employed to estimate these vectors for use in the filter. The predictor is obtained by discretizing the evolution equations (3.16).

$$\underline{H}_{k+1} = \underline{H}_k + \underline{H}_k \times \underline{\omega}_k \Delta\tau\tag{3.17}$$

$$\underline{G}_{k+1} = \underline{G}_k + \underline{G}_k \times \underline{\omega}_k \Delta\tau.\tag{3.18}$$

The correction is obtained by compensating the accelerometer outputs for vehicle motion. The acceleration measured by the instruments, expressed in gravity units, is

$$\underline{a} = \underline{k}_0 - (\dot{\underline{v}} + \underline{\omega} \times \underline{v} + \dot{\underline{\omega}} \times \underline{r}_a + \underline{\omega} \times \underline{\omega} \times \underline{r}_a) / g\tag{3.19}$$

where  $\underline{r}_a$  is the (fixed) vector from the origin of body coordinates to the accelerometer, and  $g$  is the acceleration of gravity. Compensation of the accelerometer by addition of the acceleration arising from vehicle motion estimated by the filter yields an estimate of the vector  $\underline{k}_0$  at the  $k^{\text{th}}$  step,  $\widetilde{\underline{G}}_k$ . This is a noisy estimate. Correction of (3.18) is affected by

rotation of  $\underline{G}_{k+1}$  through a fraction of the angular distance toward  $\widetilde{\underline{G}}_{k+1}$ . Let  $\underline{\Omega}_k = f \underline{G}_k \times \widetilde{\underline{G}}_k$ . Then the correction to  $\underline{G}_{k+1}$  is

$$\underline{G}_{k+1} \times \underline{\Omega}_k = -f[\widetilde{\underline{G}}_{k+1} - (\widetilde{\underline{G}}_{k+1} \cdot \underline{G}_{k+1}) \underline{G}_{k+1}], \quad (3.20)$$

since  $\underline{G}_{k+1}$  is a unit vector. ( $\underline{H}_k$  and  $\underline{G}_k$  are periodically renormalized.) Correction for (3.17) is obtained with use of the course gyro. Let the course gyro value at the  $k^{\text{th}}$  sample be denoted by  $\psi_k$ , and let  $\epsilon_k = h_1(\psi_k - \widetilde{\psi}_k)$ . Then the correction added to (3.17) is a rotation about  $\underline{G}_{k+1}$  of  $\underline{H}_{k+1}$  through the angle  $\epsilon_k$ . In addition, a correction proportional to  $\underline{G}_{k+1} \cdot \underline{H}_{k+1}$  is applied to maintain orthogonality of  $\underline{G}_k$  and  $\underline{H}_k$ . Special treatment must be given to cases where  $\widetilde{\psi}_k$  is in the neighborhood of  $\pm 180$  degrees, since incorrect course indication occurs there because of potentiometer limitations.

Trajectory increments are now obtained with the formula

$$\begin{aligned} x_{k+1} &= x_k + \underline{v}_k \cdot \underline{H}_k \Delta\tau \\ y_{k+1} &= y_k + \underline{v}_k \cdot (\underline{G}_k \times \underline{H}_k) \Delta\tau \\ z_{k+1} &= z_k + \underline{v}_k \cdot \underline{G}_k \Delta\tau. \end{aligned}$$

A correction to  $z_{k+1}$  is made by fractional movement toward the (noisy) hydrostat depth indication. Unbalanced roll torque is controlled with the roll-rate error. A complete specification of the filter equations is presented in the appendix.

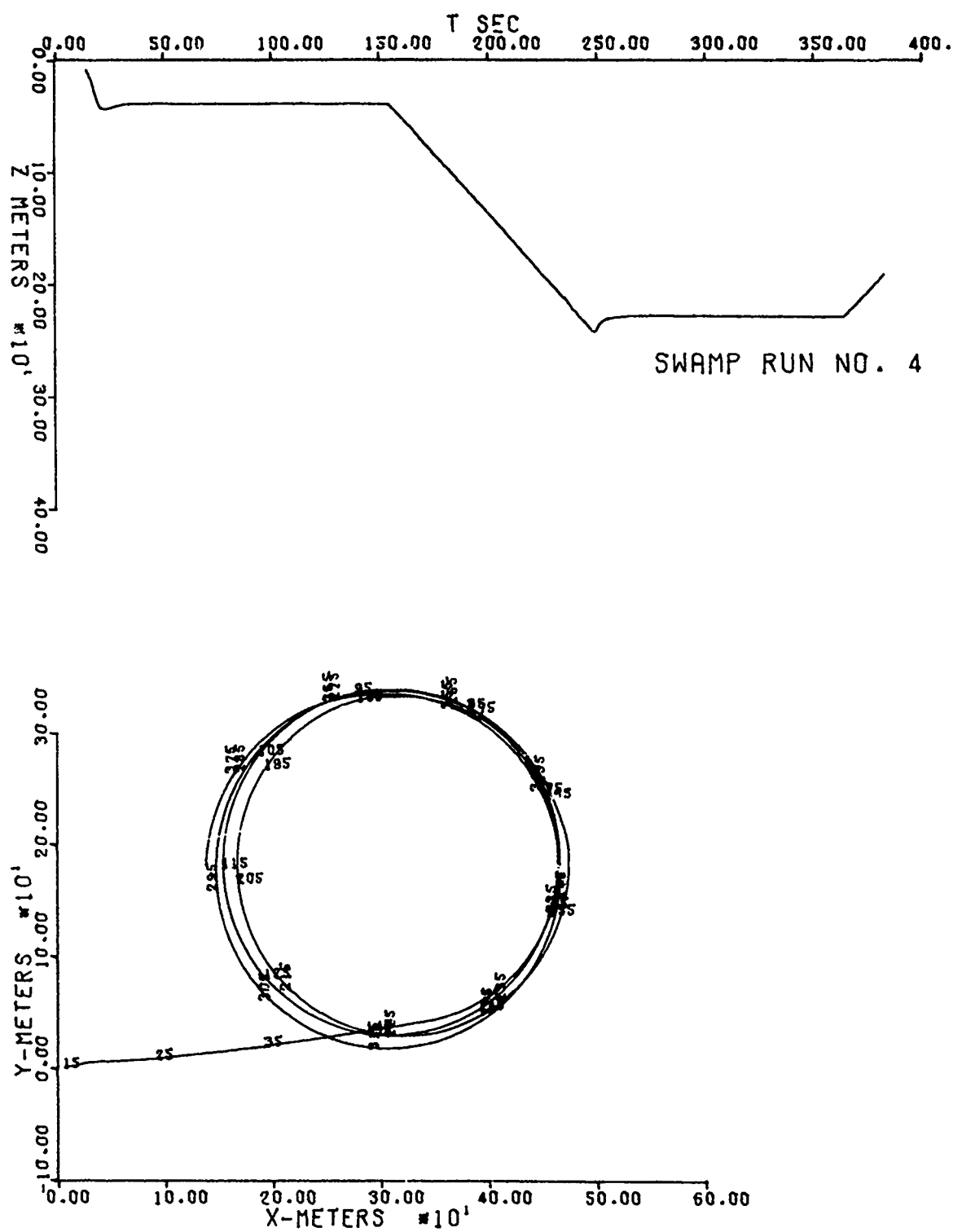
#### 4. SWAMP SEA RUN RESULTS

The filter was originally run by means of hydrodynamic coefficient data from reference 5 modified for the greater length of the SWAMP vehicle. There have been 12 successful SWAMP runs. Two of these were chosen to provide data for testing parameter estimation techniques: run no. 4 and run no. 6. Figures 4-1 and 4-2 show their respective estimated trajectories. The figures show the x-y plots, with run-time tags at 10-second intervals, and depth versus time.

Intervals were selected from these runs in which significant maneuvers occurred. From run no. 4, the following intervals were chosen: (4A) from 41 to 61 seconds, in which the vehicle, while running straight at constant depth, started turning at a rate of 4 degrees per second; (4B) from 151 to 171 seconds, in which the vehicle started to dive at a 10-degree down angle from a condition of running at constant depth and turning at 4 degrees per second; (4C) from 247 to 267 seconds, in which the vehicle pulled out of the dive and resumed circling at constant depth. From run no. 6, the following intervals were chosen: (6A) from 51 to 71 seconds, in which the SWAMP pulls out of its initial 45-degree dive angle to run at constant depth, then initiates a snake trajectory about a prescribed course; and (6B) from 136 to 156 seconds, in which the vehicle terminates the snake, executes a 90-degree turn, and commences a straight run on rate gyro control.

---

5. David W. Taylor Naval Ship Research and Development Center report 276-H-01, Model Investigation of the Submerged Stability and Control Characteristics of RETORC I, by J. H. Wolff, August 1968.



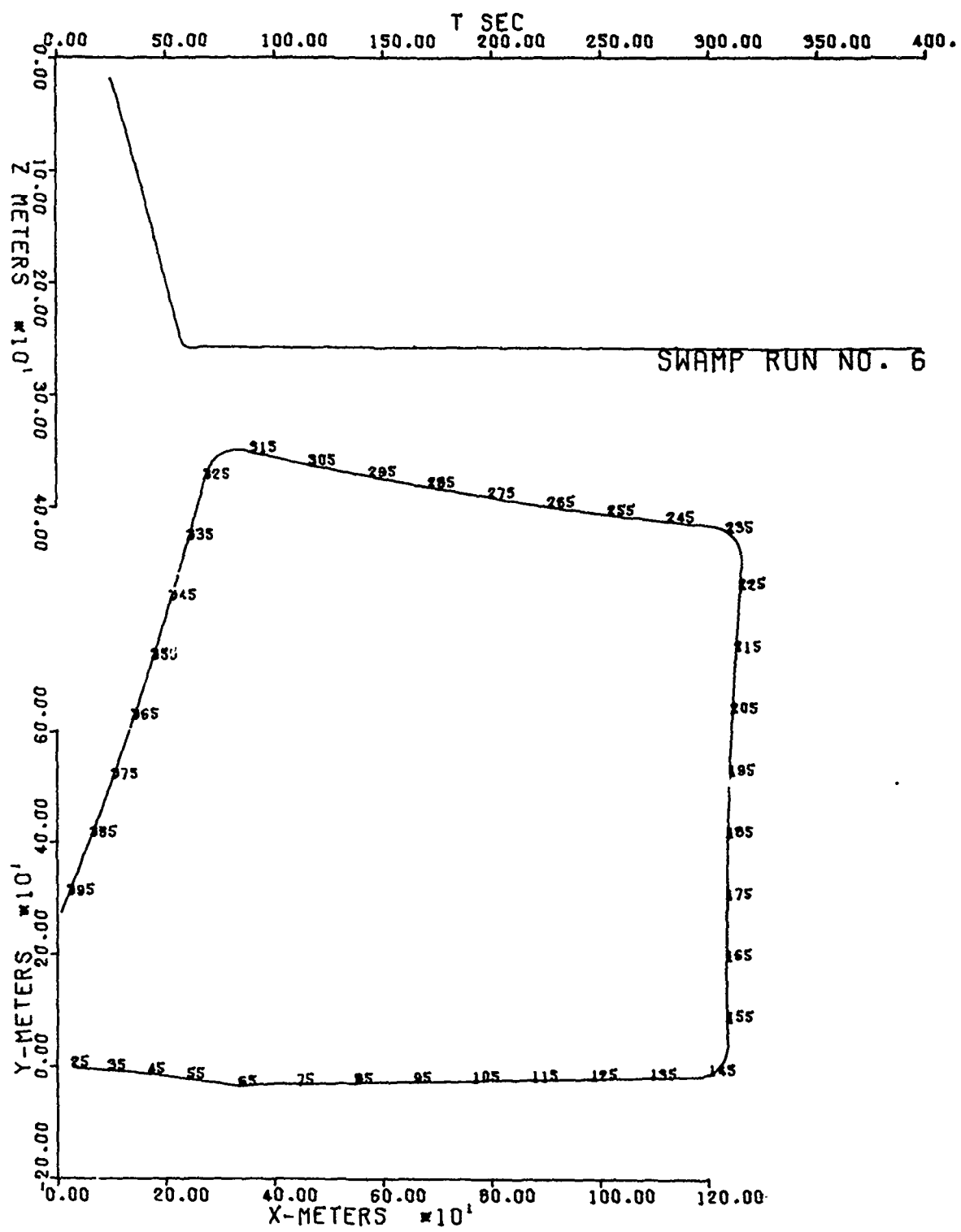


Figure 4-2. Estimated trajectory, SWAMP run no. 6.

## 5. COST FUNCTION AND ITS MINIMIZATION

The cost function was computed from the residues resulting from running the filter for one of the selected intervals. The filter was initialized 1 second before the chosen interval, using initial conditions given by the original run of the complete trajectory. The filter was then run for that 1 second, before starting to compute the cost function, to minimize the effects of initial condition transients. The cost function is a weighted sum of the squares of the rate gyro and the accelerometer residues. Let  $E_p$ ,  $E_q$ , and  $E_r$  denote the root mean square (RMS) values of the roll, pitch, and yaw rate gyro residues, respectively. Let  $E_x$ ,  $E_y$ , and  $E_z$  denote the RMS values of the accelerometer residues for the x, y, z axes, respectively. The cost function was chosen to be

$$J(\underline{\alpha}) = 0.1 E_p^2 + E_q^2 + E_r^2 + 1000 E_x^2 + 1000 E_y^2 + 100 E_z^2.$$

The weights were chosen so that the contribution of each of the RMS residues would have the same order of magnitude as the others, based on the original filter run data. The vector  $\underline{\alpha}$  was chosen to have the following components (see appendix):

$$\underline{\alpha} = (L'_{T\alpha}, Z'_{\delta e}, M'_{WB}, M'_{YB}, Z'_{qB}, r_k, K'_p, \delta_{eo}, \delta_{ro})$$

where  $\delta_{eo}$  and  $\delta_{ro}$  are biases in the control-surface measurements. The coefficient  $Z'_{WB}$  is not included because it is immaterial, as far as the linearized equations of motion are concerned, whether lift is ascribed to the body or to the tail. Consequently,  $Z'_{WB}$  retains its original estimated value throughout, as do all the other parameters in the equations of motion.

Various gradient methods (eg, steepest descent) were tried in the minimization of the cost function before it was determined that the Fletcher-Powell method would work satisfactorily.

To implement the Fletcher-Powell method, the gradient of  $J(\underline{\alpha})$  must be computed. For this purpose, small fixed increments  $h_i$  of the components of  $\underline{\alpha}$  were chosen and the central difference quotient was used as an approximate gradient.

$$g_i(\underline{\alpha}) = [J(\underline{\alpha} + h_i \underline{e}_i) - (J(\underline{\alpha} - h_i \underline{e}_i))]/(2h_i) \quad (5.1)$$

where  $\underline{e}_i$  is the unit vector for the  $i^{\text{th}}$  coordinate in  $\underline{\alpha}$  space. A sequence of matrices  $G^n$  is computed which converges to the inverse of the Hessian matrix (reference 2, p 90). At each step, a search vector

$$\underline{S}^n = -G^n g(\underline{\alpha}^n) \quad (5.2)$$

is computed. It is then required that the value  $\mu = \mu^*$ , which minimizes  $J(\underline{\alpha}^n + \mu \underline{S}^n)$ , be established. A quadratic approximation was found to be adequate, using the points  $J(\underline{\alpha}^n)$ ,  $J(\underline{\alpha}^n + \underline{S}^n)$ , and  $J(\underline{\alpha}^n + 0.5 \underline{S}^n)$ . But in any event, the range of  $K'_p$  was restricted to be between -0.01 and -0.00004 to prevent instability in the filter. The new parameter vector  $\underline{\alpha}^{n+1} = \underline{\alpha}^n + \Delta \underline{\alpha}^n$ , where  $\Delta \underline{\alpha}^n = \mu^* \underline{S}^n$  is computed, and then the matrix  $G^{n+1} = G^n + \Delta G^n$ , where

$$\Delta G^n = \frac{\Delta \underline{\alpha}^n (\Delta \underline{\alpha}^n)^T}{(\Delta \underline{\alpha}^n)^T \Delta \underline{\alpha}^n} - \frac{G^n \Delta \underline{g}^n (\Delta \underline{g}^n)^T G^n}{(\Delta \underline{g}^n)^T G^n \Delta \underline{g}^n}$$

and where  $\Delta \underline{g}^n = \underline{g}(\underline{\alpha}^{n+1}) - \underline{g}(\underline{\alpha}^n)$ . This procedure is iterated until some criterion is satisfied. In the runs made for this report,  $G^0$  was the identity matrix and the effective stopping criterion was either a specified maximum number of iterations or a maximum computer time (1 hour). A flowchart for the Fletcher-Powell method is given in figure 5-1.

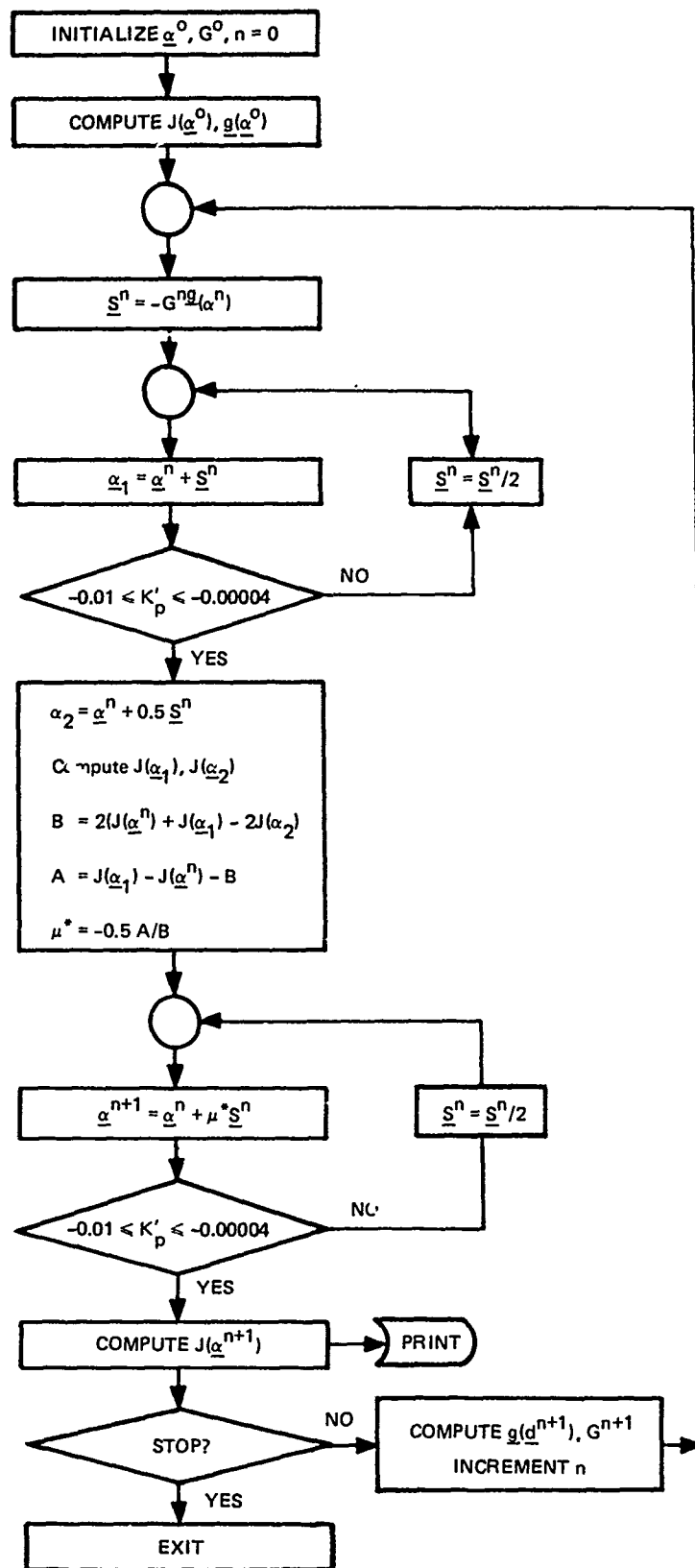


Figure 5-1. Fletcher-Powell method flowchart.

## 6. RESULTS

In all the runs, the initial parameter set was the original set which used the hydrodynamic data of reference 5 modified for the SWAMP length. Figure 6-1 shows the cost function as a function of the iteration number for runs 4A, 4B, 4C, 6A, and 6B. The process is evidently converging for each of the runs. The original parameter set and the final sets for each of the runs are presented in table 6-1. The most notable item in the results is the large values for the moment coefficients  $M'_{WB}$  and  $M'_{qB}$ . The variation of the other parameters from the original estimates was not unexpected, since they lie within tolerances usually ascribed to such data. The averages of the final values are also given. To provide a perspective of the residues of the individual rate gyros and accelerometers, the RMS values for the original and final parameter sets are tabulated in table 6-2, along with residues derived by means of the average of the final parameter sets. A comparison of the measured instrument data and that computed by the filter is shown in figures 6-2 (a, b, c, d, e, f) to 6-6 (a, b, c, d, e, f). The dotted lines represent the measured data and the solid lines are the filter output.

Run	$L'_T$	$Z'_S$	$M'_{WB}$	$M'_{qB}$	$Z'_{qB}$	$r_k$	$K'_p$	$\delta_{eo}$ (deg)	$\delta_{ro}$
4A	1.745	-0.956	1.895	-0.890	-0.123	0.337	-0.00242	0.48	-0.78
4B	1.625	-0.893	1.760	-0.678	-0.115	0.381	-0.00156	0.37	-0.40
4C	1.633	-0.914	1.682	-0.653	-0.043	0.288	-0.00084	0.22	-0.00
6A	1.878	-0.885	1.814	-0.517	-0.417	0.320	-0.00144	0.31	-0.70
6B	1.698	-1.000	1.871	-0.828	-0.231	0.295	-0.00151	0.29	-0.65
Avg	1.716	-0.930	1.804	-0.713	-0.186	0.324	-0.00155	0.33	-0.51
Orig	1.887	0.940	1.300	-0.130	-0.200	0.400	-0.00100	0.00	0.00

Table 6-1. Parameter sets (final).

Run		$E_p$	$E_q$	$E_r$	$E_x$	$E_y$	$E_z$
4A	Final	0.3378	0.1000	0.1337	0.00180	0.00610	0.02285
	Orig	0.4986	0.2941	0.2750	0.00209	0.00456	0.01355
	Avg	0.3970	0.1026	0.1540	0.00180	0.00553	0.02201
4B	Final	0.5021	0.1404	0.1580	0.00324	0.00581	0.01927
	Orig	0.8730	0.3038	0.2204	0.00419	0.00720	0.02001
	Avg	0.6466	0.1222	0.1606	0.00320	0.00662	0.01798
4C	Final	1.297	0.1807	0.2230	0.00404	0.01147	0.02164
	Orig	1.698	0.4410	0.2450	0.00713	0.01625	0.02389
	Avg	1.439	0.1686	0.1798	0.00413	0.01267	0.02123
6A	Final	0.6085	0.1606	0.1610	0.00400	0.00536	0.01713
	Orig	0.7030	0.4129	0.3104	0.00446	0.00620	0.01454
	Avg	0.6125	0.1583	0.1560	0.00540	0.00761	0.01849
6B	Final	0.8063	0.1213	0.1502	0.00251	0.00969	0.01868
	Orig	0.9362	0.3130	0.3201	0.00202	0.00942	0.01671
	Avg	0.8262	0.1259	0.1629	0.00256	0.00944	0.01909

Table 6-2. RMS instrument residues.  
(Rate gyros deg/s, acceleration, g)

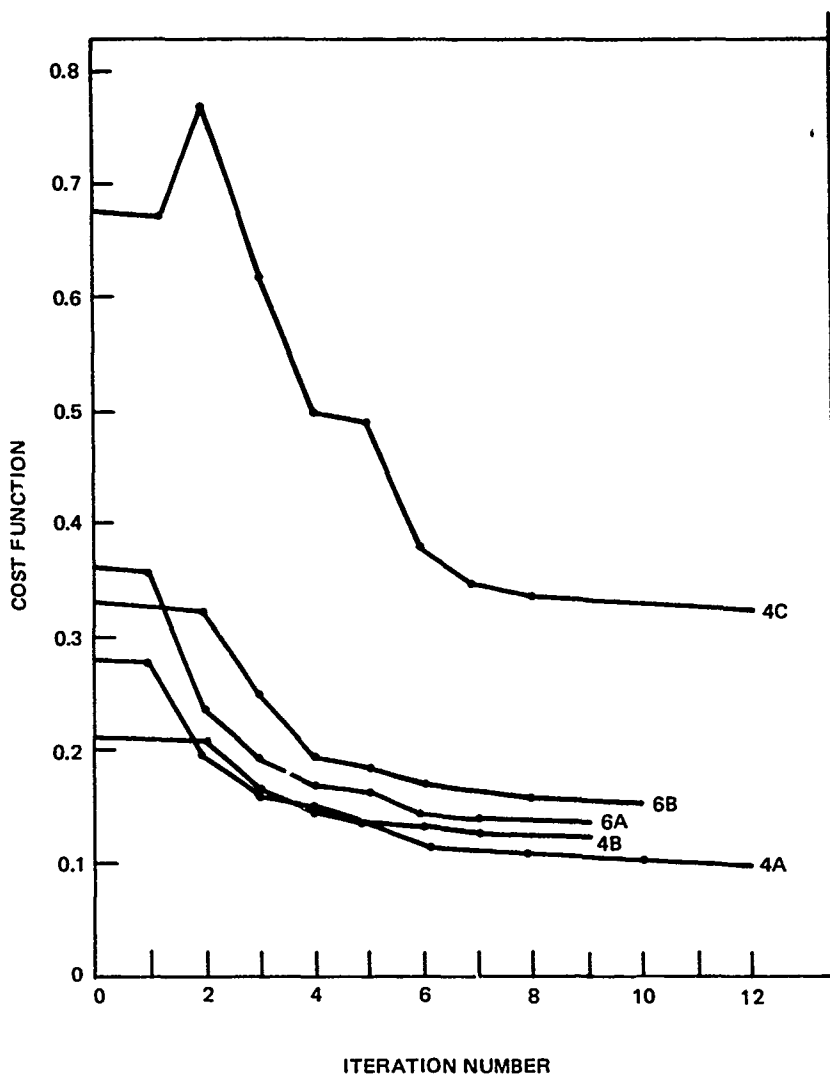


Figure 6-1. Cost function versus iteration number.

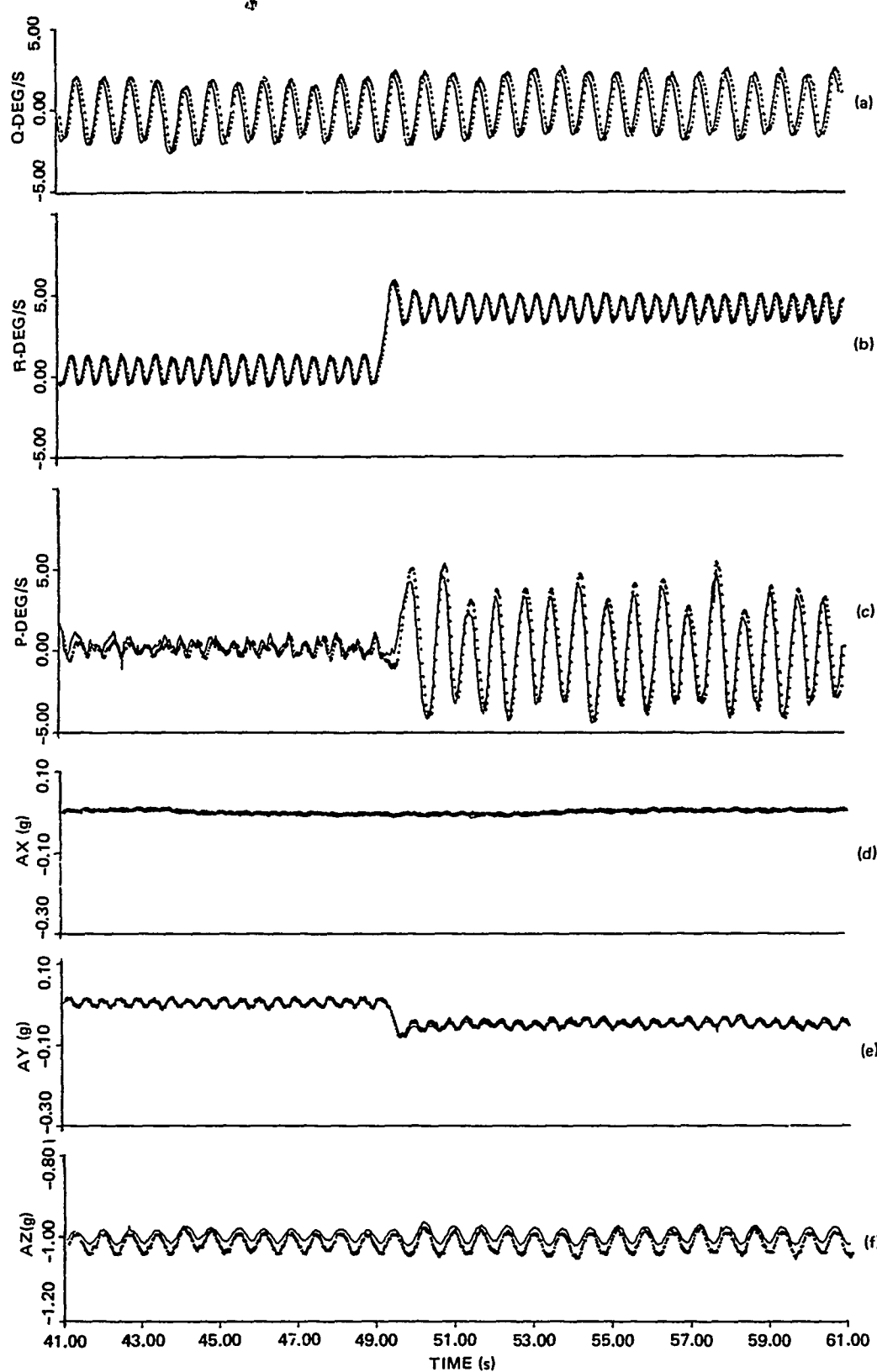


Figure 6-2. Swamp run no. 4.

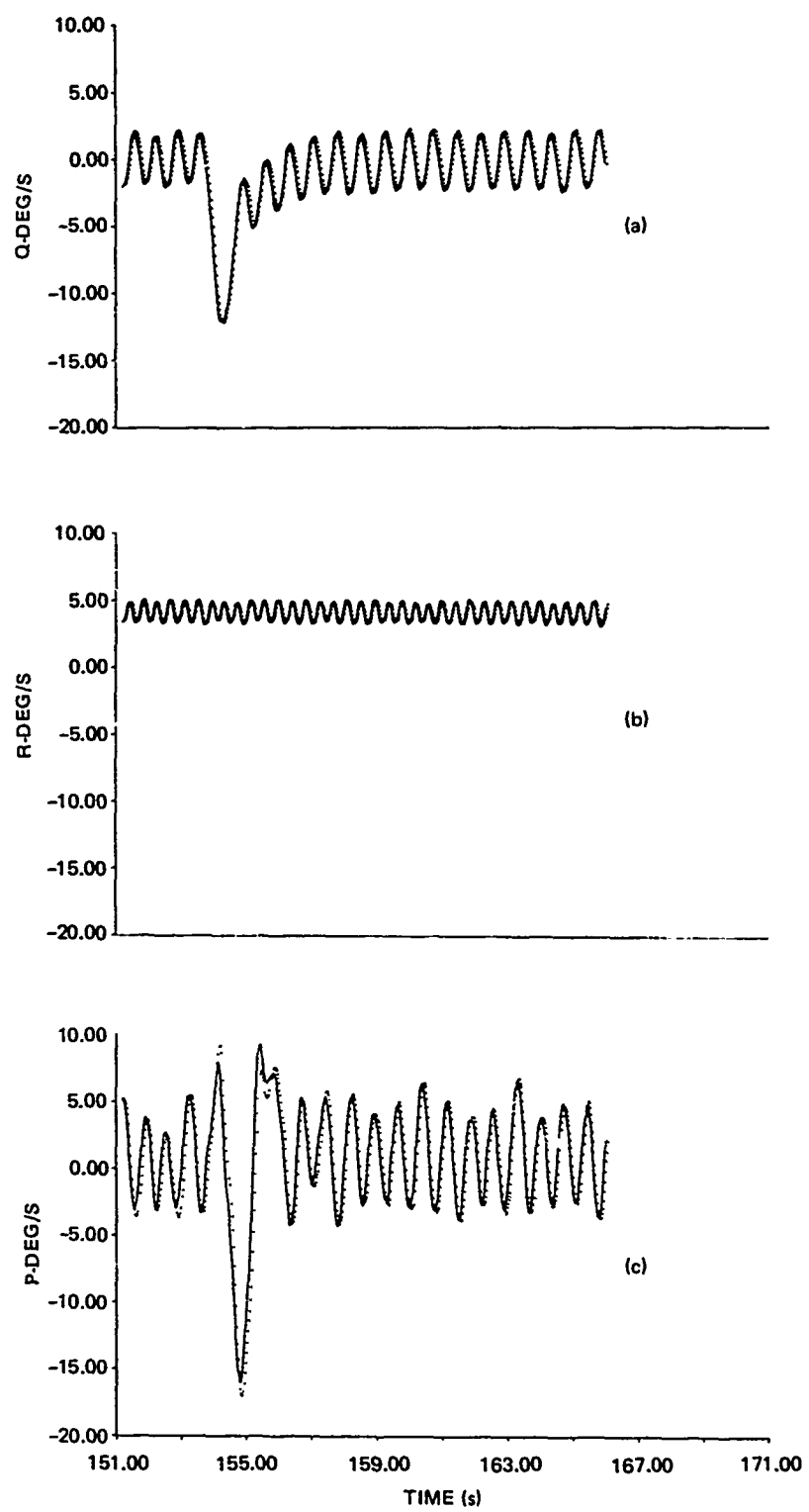


Figure 6-3. Swamp run no: 4.

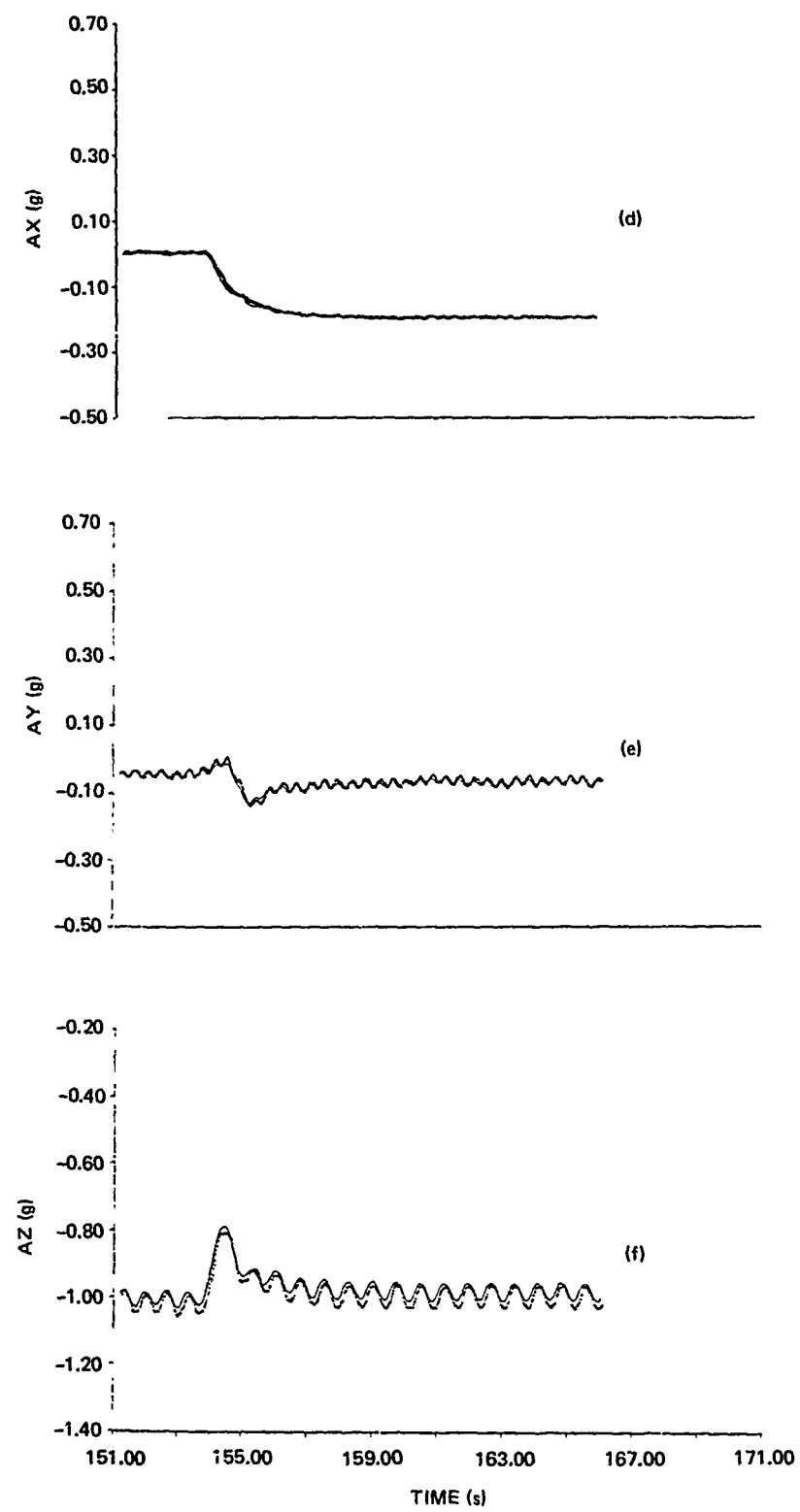


Figure 6-3. Continued.

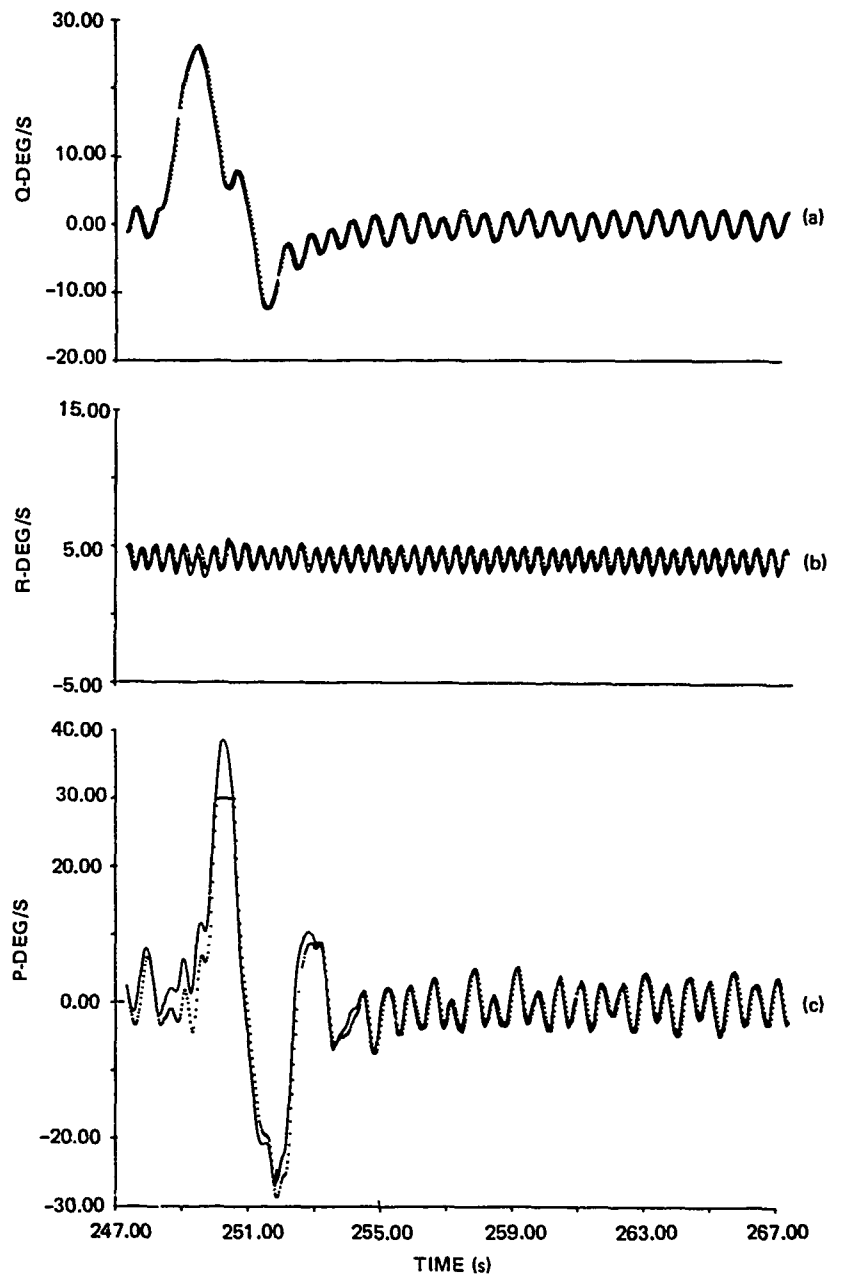


Figure 6-4. Swamp run no. 4.

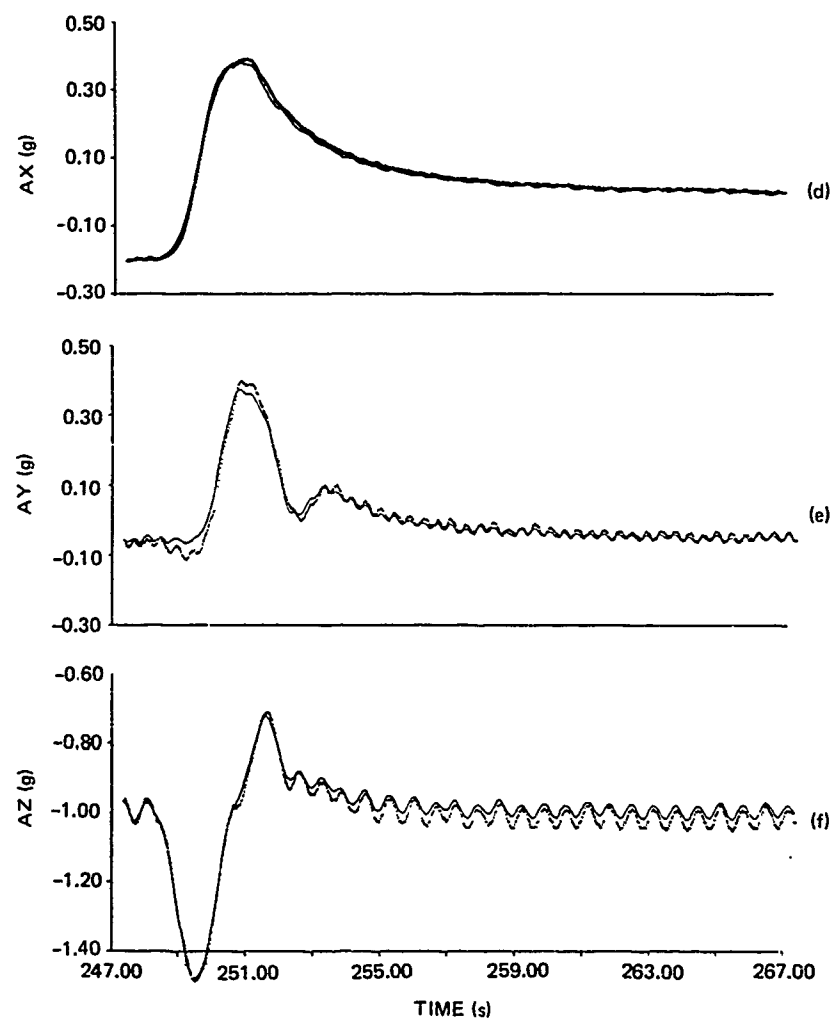


Figure 6-4. Continued.

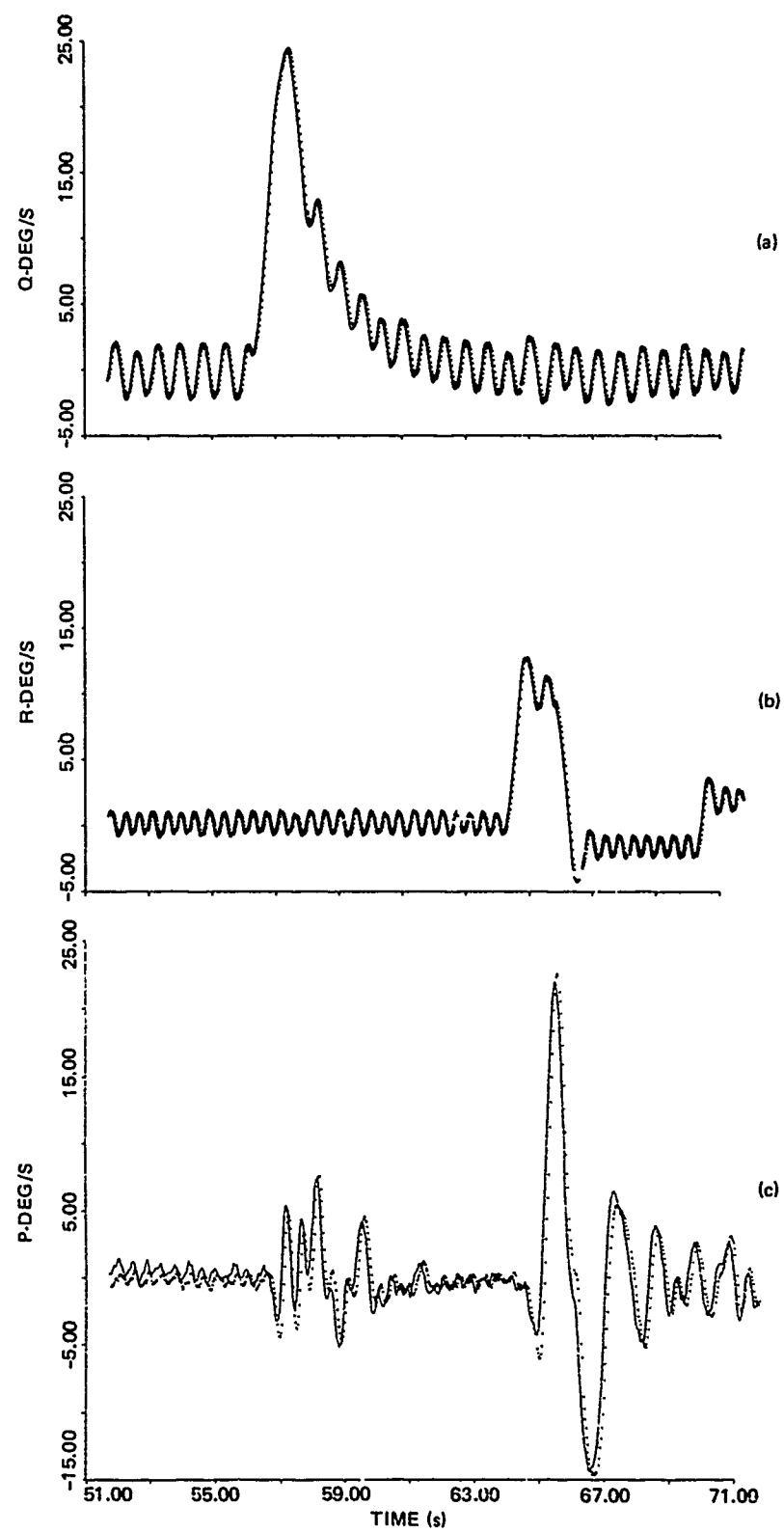


Figure 6-5. Swamp run no. 6.

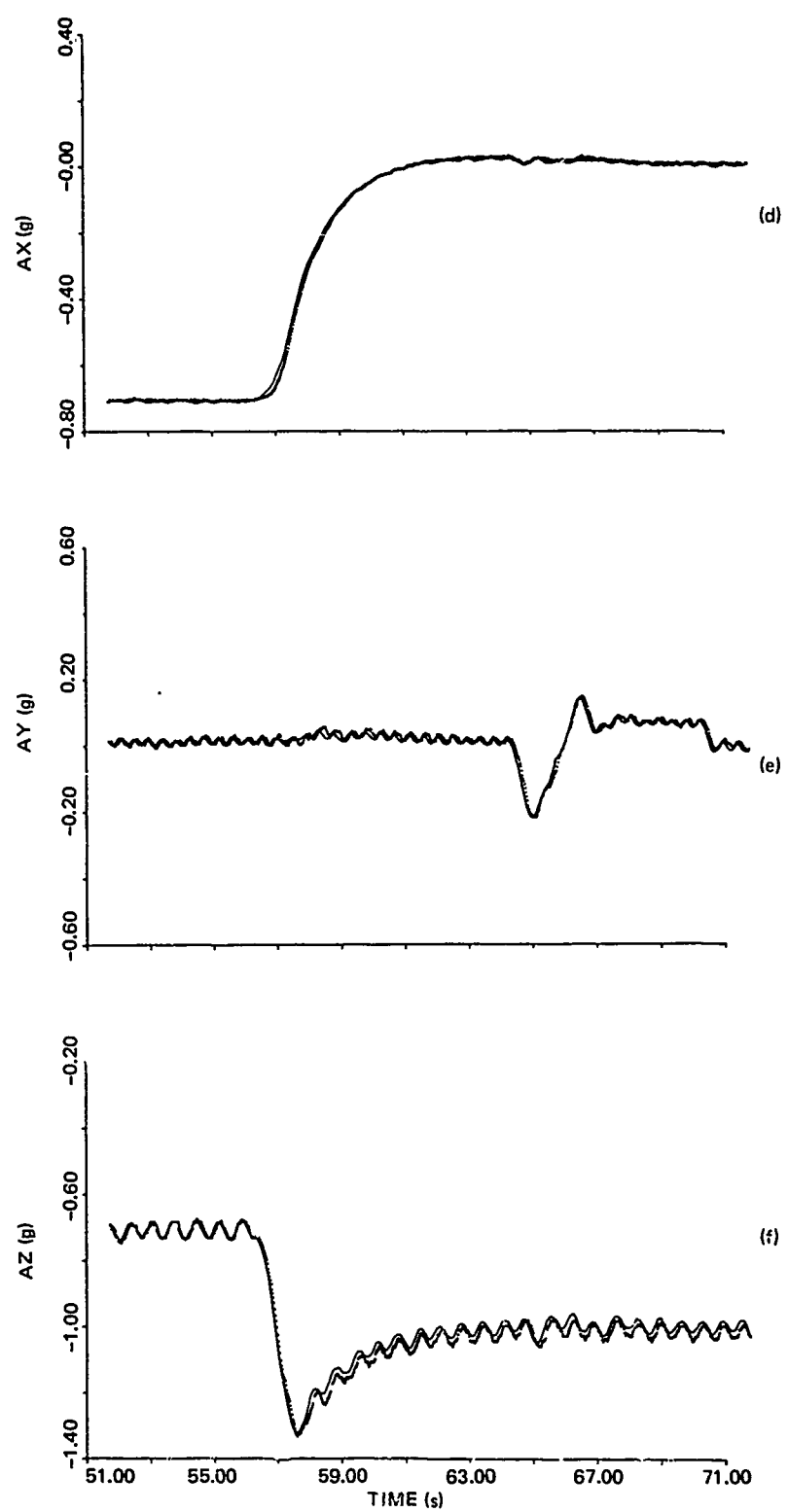


Figure 6-5. Continued.

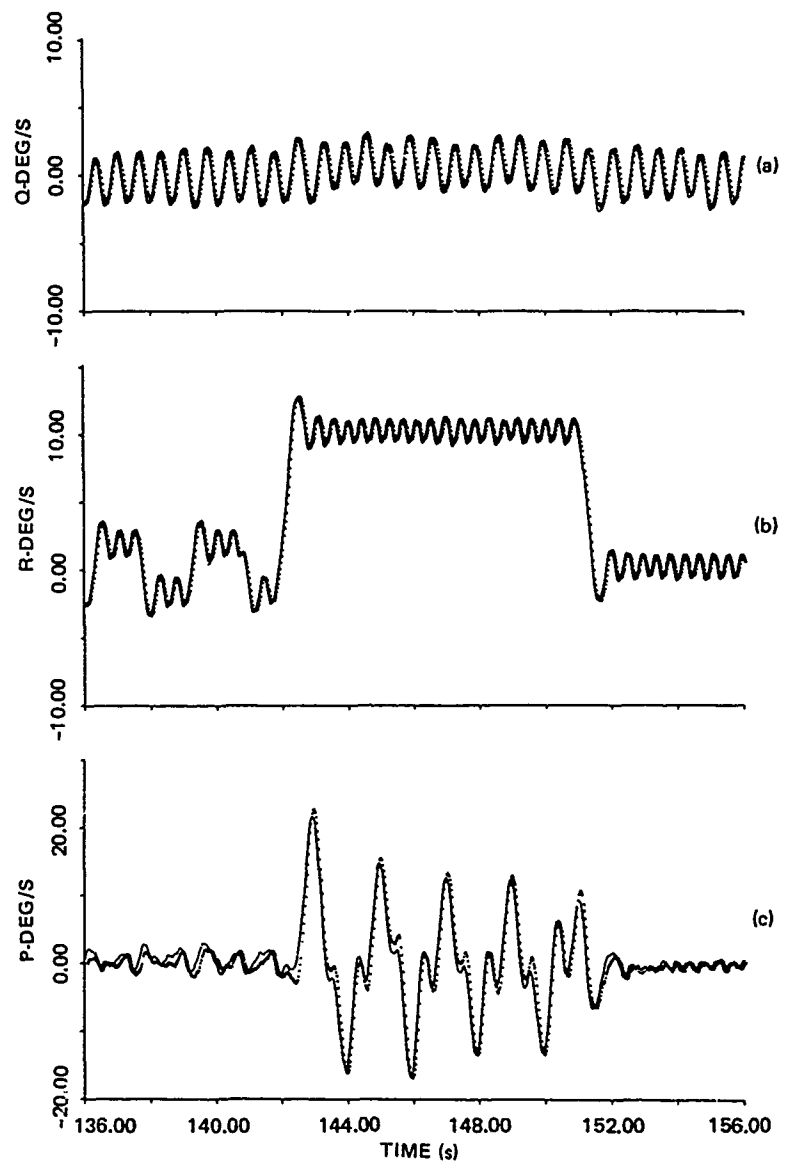


Figure 6-6. Swamp run no. 6.

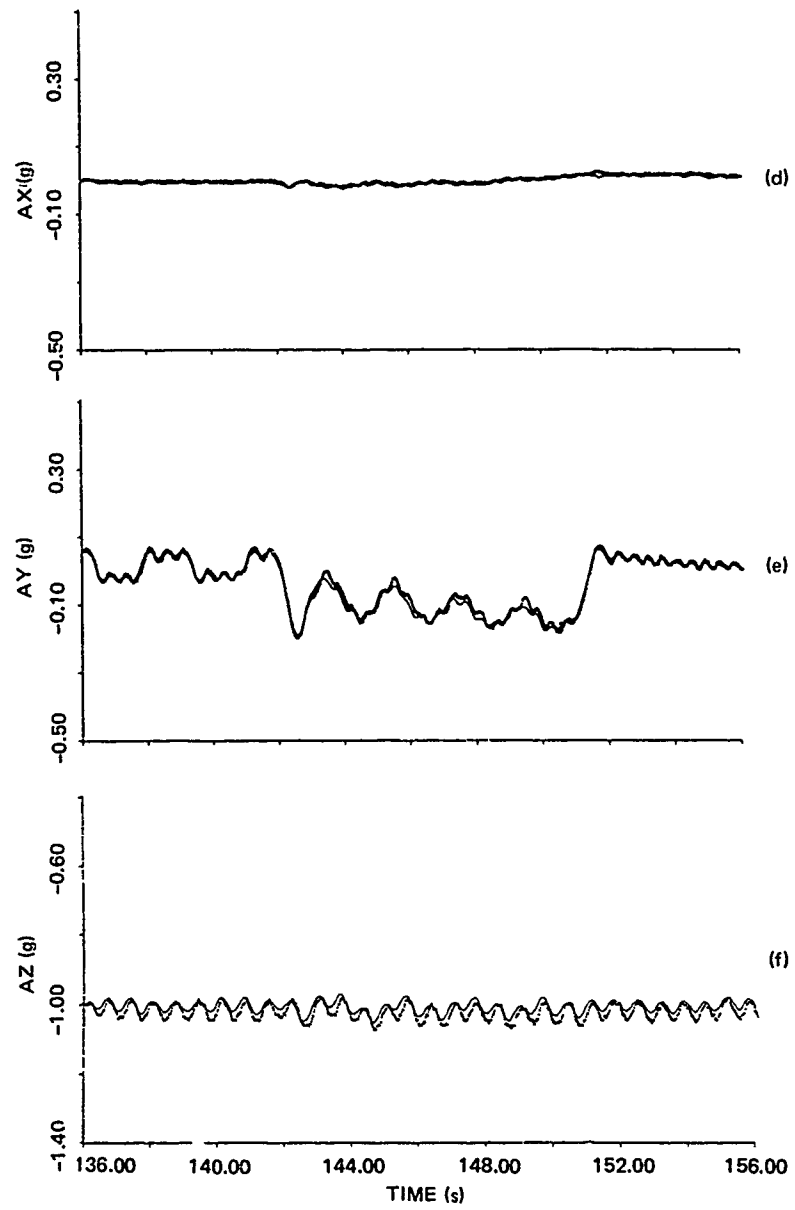


Figure 6-6. Continued.

## 7. CONCLUSIONS AND RECOMMENDATIONS

1. The implementation of the Fletcher-Powell method used here is a practical technique for estimating hydrodynamic coefficients from sea-run data.
2. Further work on post-run analysis should include:
  - a. Analysis of the data to estimate correlation matrices. This is necessary if optimal Kalman filters and maximum-likelihood identification are to be implemented.
  - b. Improvement of the system model by identification of nonlinear effects in yaw, pitch, and roll coupling.
  - c. Further development of digital recording and playback equipment for use in torpedo guidance and control development, test, and evaluation.

## REFERENCES

1. National Aeronautics and Space Administration TN D-7647, Parameter Estimation Techniques and Applications in Aircraft Flight Testing, April 1974.
2. Sage, A. P., and J. C. Melsa, System Identification, Academic Press, 1971.
3. Aoki, M., Optimization of Stochastic Systems, Academic Press, 1967.
4. Naval Ordnance Test Station (Pasadena) NAVORD report 2090, Motion Equations for Torpedoes, by L. Lopes, 12 February 1954.
5. David W. Taylor Naval Ship Research and Development Center report 276-H-01, Model Investigation of the Submerged Stability and Control Characteristics of RETORC I, by J. H. Wolff, August 1968.
6. Available to qualified requesters.

## APPENDIX: FILTER EQUATIONS

The instruments used in the measurements are the same as in the control system of the Mk 46 Mod 1 torpedo. The rate gyros and accelerometers have a second-order response characteristic with a natural frequency of about 27 Hz and a damping ratio of about 0.7. Let the operator  $L$  be identified by

$$L = 1 + (2\xi/\omega_0) D + (1/\omega_0^2) D^2 \quad (A.1)$$

where  $D = d/dt$ . Then the rate gyro equations are

$$\begin{aligned} (a) \quad Lp_g &= \hat{p} \\ (b) \quad Lq_g &= \hat{q} \\ (c) \quad Lr_g &= \hat{r} \end{aligned} \quad (A.2)$$

where  $p_g$ ,  $q_g$ , and  $r_g$  are, respectively, the roll, pitch, and yaw rate gyro outputs and the caret indicates that the state variable input is limited to 1 radian per second.

The accelerometers have a similar response. Let  $A_x$ ,  $A_y$ , and  $A_z$  be the  $x$ ,  $y$ , and  $z$  accelerometer outputs, respectively. Then

$$\begin{aligned} (a) \quad LA_x &= a_x \\ (b) \quad LA_y &= a_y \\ (c) \quad LA_z &= a_z \end{aligned} \quad (A.3)$$

where

$$\begin{aligned} (a) \quad a_x &= G_1 - [u + wq - vr + qz_x - ry_x + p(qy_x + rz_x) + (q^2 + r^2)x_x]/g \\ (b) \quad a_y &= G_2 - [v + ur = wp + rx_y - pz_y + q(rz_y + pz_y) - (r^2 + p^2)y_y]/g \\ (c) \quad z &= G_3 - [w + vp - uq + py_2 - qx_z + z(px_z + qy_z) - (p^2 + q^2)z_z]/g \end{aligned} \quad (A.4)$$

and where  $(x_x, y_x, z_x)$ ,  $(x_y, y_y, z_y)$ , and  $(x_z, y_z, z_z)$  are the respective coordinates of the  $x$ ,  $y$ , and  $z$  accelerometers.

The motion equations for the first-stage predictor are

$$\begin{aligned} (a) \quad m_L \dot{u} &= \text{THRUST} - \text{DRAG} + (W - B) G_1 - m_T(wq - vr) + mz_G pr \\ (b) \quad m_T \dot{w} &= Z_{qB} uq + Z_{wB} uw + Z_{wD} |w| w + Z_T + (W - B) G_3 \\ (c) \quad m_T \dot{v} &= Y_{mB} ur + Y_{vB} uv + Y_{vD} |v| v + Y_{TU} + Y_{TL} + (W - B) G_2 + mz_G (\dot{p} - qr) \\ (d) \quad J_x \dot{p} &= K_p up + r_k(Y_{TU} - Y_{TL}) + mz_G (\dot{v} + ur - wp) - Wz_G G_2 + K_o \\ (e) \quad J_y \dot{q} &= M_{wB} uw + M_{qB} uq - x_T Z_T - W(x_G G_3 - Z_G G_1) - mz_G (\dot{u} + wq - vr) \\ &\quad + (J_y - J_x) pr \\ (f) \quad J_z \dot{r} &= N_{vB} uv + N_{rB} ur + x_T(Y_{TU} + Y_{TL}) + Wx_G G_2 - (J_y - J_x) pq \end{aligned} \quad (A.5)$$

where

$$Z_{qB} = \rho/2 A \ell Z'_{qB} + m_L, \quad Z_{wB} = \rho/2 A Z'_{wB},$$

$$\begin{aligned}
Z_{WD} &= -\rho/2 A C_{DC}, \quad M_{WB} = \rho/2 A \ell M'_{WB}, \\
M_{QB} &= \rho/2 A \ell^2 M'_{QB}, \quad Y_{rB} = -Z_{QB}, \quad Y_{vB} = Z_{WB}, \\
Y_{vD} &= Z_{WD}, \quad N_{vB} = -M_{WB}, \quad N_{rB} = M_{QB}, \\
K_p &= \rho/2 A \ell^2 K'_p.
\end{aligned}$$

THRUST is a homogeneous quadratic function of  $u$  and RPS, propeller rotational speed, that was fitted to empirical data for the RETORC I propellers.

$$\text{THRUST} = -0.0136 u^2 - 0.659u \cdot \text{RPS} + 2.07 \text{ RPS}^2 \quad (\text{A.6})$$

$$\text{DRAG} = \rho/2 A (C_D u^2 + 0.676u - 3.38), \quad u > 4. \quad (\text{A.7})$$

The drag coefficient  $C_D$  was adjusted to give a speed consistent with the observed dive rate of SWAMP.

The tail lift terms are given by reference 6.

$$Z_T = \begin{cases} -\rho/2 A L'_{T\alpha} w_T \sqrt{u^2 + 6.44 w_T^2}, & |\alpha_T| \leq 40^\circ \\ -\rho/2 A (1.4) w_T \sqrt{u^2 + w_T^2}, & |\alpha_T| > 40^\circ \end{cases} \quad (\text{A.8})$$

where  $w_T = w - x_T q - C_\delta u \delta_e$ ,  $C_\delta = Z'_{\delta_e} / L'_{T\alpha}$

$$Y_{TU} = \begin{cases} -\rho/4 A L'_{T\alpha} v_{TU} \sqrt{u^2 + 6.44 v_{TU}^2}, & |\beta_{TU}| \leq 40^\circ \\ -\rho/4 A (1.4) v_{TU} \sqrt{u^2 + v_{TU}^2}, & |\beta_{TU}| > 40^\circ \end{cases} \quad (\text{A.9})$$

$$Y_{TL} = \begin{cases} -\rho/4 A L'_{T\alpha} v_{TL} \sqrt{u^2 + 6.44 v_{TL}^2}, & |\beta_{TL}| \leq 40^\circ \\ -\rho/4 A (1.4) v_{TL} \sqrt{u^2 + v_{TL}^2}, & |\beta_{TL}| > 40^\circ \end{cases} \quad (\text{A.10})$$

where

$$v_{TU} = v + x_T r + C_\delta u \delta_u$$

$$v_{TL} = v + x_T r + C_\delta u \delta_L$$

The evolution equations for the direction cosines are

$$(a) \quad \dot{G}_1 = r G_2 - q G_3$$

$$(b) \quad \dot{G}_2 = p G_3 - r G_1$$

$$(c) \quad \dot{G}_3 = q G_1 - p G_2$$

---

6. Available to qualified requesters.

(d)  $\dot{H}_1 = rH_2 - qH_3$   
 (e)  $\dot{H}_2 = pH_3 - rH_1$   
 (f)  $\dot{H}_3 = qH_1 = pH_2.$  (A.11)

The equations for the geographic x-y coordinates and depth z are

(a)  $\dot{x} = uH_1 + vH_2 + wH_3$   
 (b)  $\dot{y} = uF_1 + vF_2 + wF_3$   
 (c)  $\dot{z} = uG_1 + vG_2 + wG_3$  (A.12)

where  $\underline{F} = \underline{G} \times \underline{H}.$

The corrector equation for the vector (3.3) is in accordance with (3.13). The vector  $\widetilde{H}_{k+1}$  is the output of equations (A.2) at the  $k^{\text{th}}$  step. When a rate gyro measurement saturates, the corresponding correction is set to zero.

The direction cosine vector  $\underline{Q}$  is not corrected for the first 10 seconds after water entry to allow time for the initial transient to pass. After this time, the body acceleration terms of equations (A.4) are used to compensate the measured accelerations and thereby provide an indication of the gravitational vector  $\underline{G}_I.$  The vector  $\underline{G}$  is then corrected according to the equation

$$\underline{G}_{k+1} = \widetilde{\underline{G}}_k + 0.1 (\underline{G}_I - \underline{G}_k) \quad (\text{A.13})$$

where  $\underline{G}_k$  is the predicted value using (A.11).

The  $\underline{H}$  vector is corrected by the equation

$$\underline{H}_{k+1} = \underline{H}_{k+1} + \alpha \underline{G}_{k+1} \times \widetilde{\underline{H}}_{k+1} - \beta \underline{G}_{k+1} \quad (\text{A.14})$$

where

$$\alpha = 0.1 (\Psi_{k+1} - \Psi_I)$$

$$\beta = 0.1 (\underline{G}_{k+1} \cdot \underline{H}_{k+1}),$$

$\widetilde{\Psi}_{k+1}$  being the course angle determined by  $\underline{G}_{k+1}$  and  $\underline{H}_{k+1}$ , and  $\Psi_I$  the current course gyro measurement. When the course is in the neighborhood of  $\pm 180^{\circ}$ , the gyro does not give a correct course measurement. During this period,  $\alpha$  is set at zero.

Depth is corrected according to the hydrostat measurement by

$$z_{k+1} = \widetilde{z}_{k+1} + 0.01 (z_I - \widetilde{z}_{k+1}) \quad (\text{A.15})$$

where  $z_I$  is the current hydrostat indication of depth and  $z_{k+1}$  is the depth predicted by (A.12c).

Unbalanced roll torque is controlled by the difference between measured and estimated roll rate.

$$K_{o,k+1} = K_{o,k} + 0.5 (p_G - P_{gk+1})$$

where  $p_G$  is the current roll rate measurement, and  $P_{gk+1}$  is the current computed rate gyro output.